JCI The Journal of Clinical Investigation

Pancreatic GLP-1 receptor activation is sufficient for incretin control of glucose metabolism in mice

Benjamin J. Lamont, … , Herbert Gaisano, Daniel J. Drucker

J Clin Invest. 2012;122(1):388-402. https://doi.org/10.1172/JCI42497.

Research Article Endocrinology

Glucagon-like peptide-1 (GLP-1) circulates at low levels and acts as an incretin hormone, potentiating glucose-dependent insulin secretion from islet β cells. GLP-1 also modulates gastric emptying and engages neural circuits in the portal region and CNS that contribute to GLP-1 receptor–dependent (GLP-1R–dependent) regulation of glucose homeostasis. To elucidate the importance of pancreatic GLP-1R signaling for glucose homeostasis, we generated transgenic mice that expressed the human GLP-1R in islets and pancreatic ductal cells (Pdx1-hGLP1R:*Glp1r*$^{-/-}$ mice). Transgene expression restored GLP-1R–dependent stimulation of cAMP and Akt phosphorylation in isolated islets, conferred GLP-1R–dependent stimulation of β cell proliferation, and was sufficient for restoration of GLP-1–stimulated insulin secretion in perifused islets. Systemic GLP-1R activation with the GLP-1R agonist exendin-4 had no effect on food intake, hindbrain c-fos expression, or gastric emptying but improved glucose tolerance and stimulated insulin secretion in Pdx1-hGLP1R:*Glp1r*$^{-/-}$ mice. i.c.v. GLP-1R blockade with the antagonist exendin$^{(9–39)}$ impaired glucose tolerance in WT mice but had no effect in Pdx1-hGLP1R:*Glp1r*$^{-/-}$ mice. Nevertheless, transgenic expression of the pancreatic GLP-1R was sufficient to normalize both oral and i.p. glucose tolerance in *Glp1r*$^{-/-}$ mice. These findings illustrate that low levels of endogenous GLP-1 secreted from gut endocrine cells are capable of augmenting glucoregulatory activity via pancreatic GLP-1Rs independent of communication with neural pathways.

Pancreatic GLP-1 receptor activation is sufficient for incretin control of glucose metabolism in mice

Benjamin J. Lamont,[1] Yazhou Li,[1] Edwin Kwan,[2] Theodore J. Brown,[3] Herbert Gaisano,[2] and Daniel J. Drucker[1]

[1]Department of Medicine, Samuel Lunenfeld Research Institute, Mount Sinai Hospital, University of Toronto, Toronto, Ontario, Canada.
[2]Department of Physiology, University Health Network, University of Toronto, Toronto, Ontario, Canada.
[3]Department of Physiology, Samuel Lunenfeld Research Institute, Mount Sinai Hospital, University of Toronto, Toronto, Ontario, Canada.

Glucagon-like peptide-1 (GLP-1) circulates at low levels and acts as an incretin hormone, potentiating glucose-dependent insulin secretion from islet β cells. GLP-1 also modulates gastric emptying and engages neural circuits in the portal region and CNS that contribute to GLP-1 receptor–dependent (GLP-1R–dependent) regulation of glucose homeostasis. To elucidate the importance of pancreatic GLP-1R signaling for glucose homeostasis, we generated transgenic mice that expressed the human GLP-1R in islets and pancreatic ductal cells (Pdx1-hGLP1R:*Glp1r*$^{-/-}$ mice). Transgene expression restored GLP-1R–dependent stimulation of cAMP and Akt phosphorylation in isolated islets, conferred GLP-1R–dependent stimulation of β cell proliferation, and was sufficient for restoration of GLP-1–stimulated insulin secretion in perifused islets. Systemic GLP-1R activation with the GLP-1R agonist exendin-4 had no effect on food intake, hindbrain c-fos expression, or gastric emptying but improved glucose tolerance and stimulated insulin secretion in Pdx1-hGLP1R:*Glp1r*$^{-/-}$ mice. i.c.v. GLP-1R blockade with the antagonist exendin$^{(9-39)}$ impaired glucose tolerance in WT mice but had no effect in Pdx1-hGLP1R:*Glp1r*$^{-/-}$ mice. Nevertheless, transgenic expression of the pancreatic GLP-1R was sufficient to normalize both oral and i.p. glucose tolerance in *Glp1r*$^{-/-}$ mice. These findings illustrate that low levels of endogenous GLP-1 secreted from gut endocrine cells are capable of augmenting glucoregulatory activity via pancreatic GLP-1Rs independent of communication with neural pathways.

Introduction

Multiple tissues contribute to the maintenance of blood glucose levels after nutrient ingestion, with liver and muscle responsible for disposal of the majority of excess glucose in the postprandial state (1). In these tissues, glucose can either be used as a fuel for metabolism or stored in the form of glycogen for later use. Excess nutrients are also stored in adipose tissue. Insulin secreted from pancreatic β cells in response to nutrient ingestion regulates many of these processes. However, the pancreas is only one of many sites important for nutrient sensing and communication of metabolic signals regulating energy assimilation and storage (2).

Our understanding of adipose tissue has evolved from a passive site of fuel storage to a metabolically active tissue secreting adipokines, such as leptin, adiponectin, and resistin, that in turn regulate energy homeostasis (3, 4). In addition to sensing hormonal signals from peripheral tissues, the brain also senses and responds to nutrients directly and receives signals from afferent nerves reflecting peripheral inputs into glucose metabolism (5, 6). An important source of these afferent inputs is the intestine, an organ originating signals arising from enteral nutrients within minutes of food ingestion (7, 8) via an extensive neural network. The gut also releases multiple hormones (9) that in turn relay information via endocrine and neural circuits to the brain, pancreas, and other tissues controlling nutrient assimilation.

There is considerable interest in understanding how gut-derived signals communicate with the β cell to promote insulin secretion. Glucose-dependent insulinotropic peptide (GIP) and glucagon-like peptide-1 (GLP-1) are released from enteroendocrine cells of the intestine after food ingestion and stimulate insulin secretion in a glucose-dependent manner (10). However, due to the rapid cleavage of these peptide hormones by dipeptidyl peptidase 4, only a small percentage of the total GIP or GLP-1 secreted by the intestine actually reaches β cells in active form, rendering uncertain the mechanisms underlying the classical incretin concept (11, 12). GLP-1 also exerts inhibitory actions on food intake and gastric emptying, involving activation of neurons within the hypothalamus (13–15). Reduced feeding activity can be seen after either i.c.v. or peripheral administration of GLP-1 receptor (GLP-1R) agonists, and CNS GLP-1R blockade increases food intake (16, 17), suggesting that even low basal levels of GLP-1R signaling control nutrient ingestion. Intriguingly, peripheral administration of high molecular weight GLP-1R agonists also reduces food intake (14, 18) and promotes weight loss (19), implying that signals originating from peripheral GLP-1R activation can be relayed to the brain.

Accumulating evidence suggests that activation of extrapancreatic GLP-1Rs represents an important mechanism underlying actions of GLP-1 on glucose metabolism (2, 20). The hepatoportal region is exposed to relatively higher levels of active GLP-1, and signals arising from the hepatoportal GLP-1R facilitate glucose clearance independent of changes in insulin secretion (21, 22). Moreover,

Authorship note: Benjamin J. Lamont and Yazhou Li contributed equally to this work.

Conflict of interest: Daniel J. Drucker has received more than $10,000 in speaking, consulting, and advisory board fees in the past 12 months from Eli Lilly and Co., Merck & Co. Inc., and Novo Nordisk. Benjamin J. Lamont was supported in part through an unrestricted grant in incretin biology from Merck & Co. Inc. to Mount Sinai Hospital.

Citation for this article: *J Clin Invest*. 2012;122(1):388–402. doi:10.1172/JCI42497.

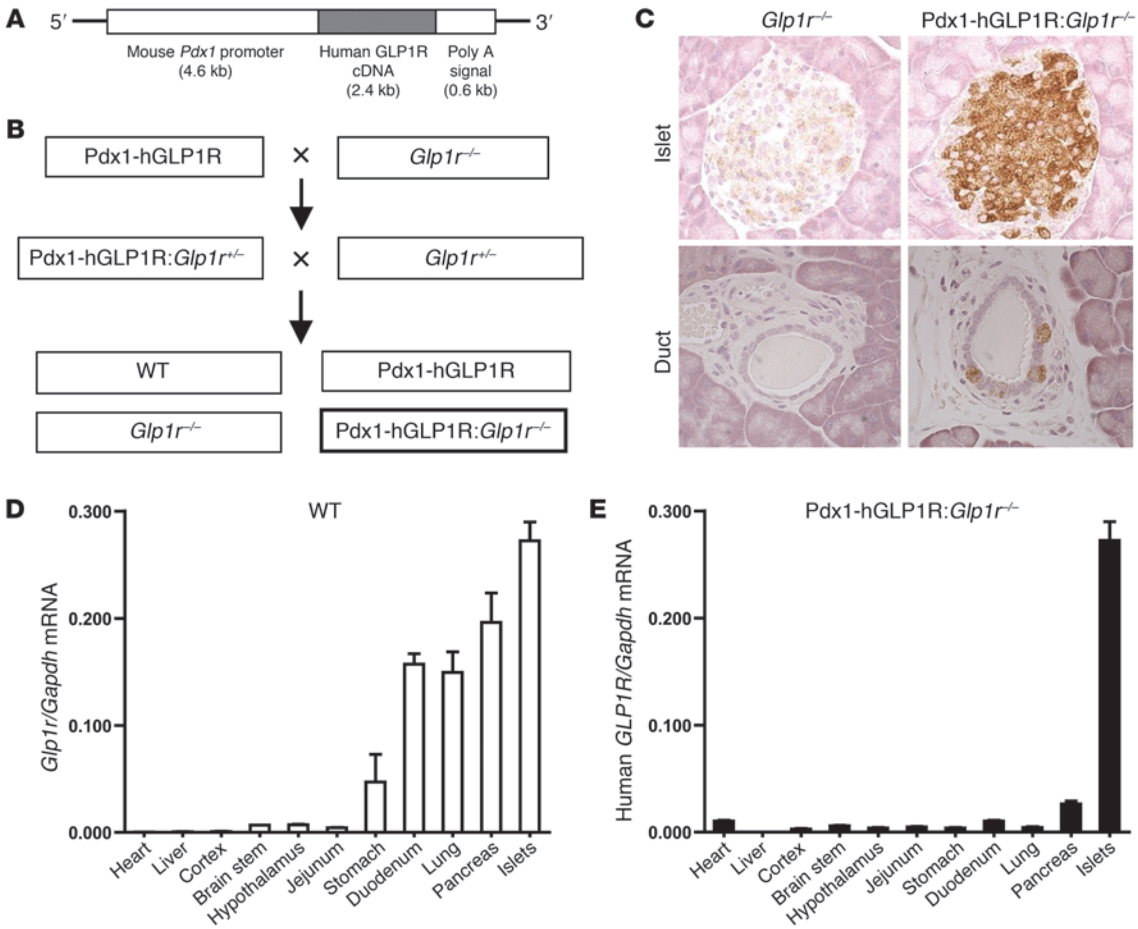

Figure 1

Transgenic rescue of pancreatic GLP-1R expression in the *Glp1r*$^{-/-}$ mouse. (**A**) A gene construct containing the mouse *Pdx1* promoter sequence, the human GLP-1R cDNA, and a poly A signal was used to generate Pdx1-hGLP1R transgenic mice. (**B**) To restore the expression of GLP-1R in pancreatic ductal and β cells, Pdx1-hGLP1R transgenic mice were crossed with *Glp1r*$^{-/-}$ mice to generate Pdx1-hGLP1R:*Glp1r*$^{-/-}$ mice. (**C**) Immunohistochemistry detected the GLP-1R in pancreatic islets and ducts from Pdx1-hGLP1R:*Glp1r*$^{-/-}$ mice but not *Glp1r*$^{-/-}$ littermates. Original magnification, ×20. Real-time quantitative PCR analysis determined the levels of endogenous (**D**) *Glp1r* mRNA (Taqman assay Mm01351008_m1) in WT mice and (**E**) human *GLP1R* (transgene – Hs01006332) mRNA in Pdx1-hGLP1R:*Glp1r*$^{-/-}$ mice. Results were normalized to *Gapdh* (Mm03302249) (n = 3–7).

GLP-1 is also produced in brain stem and hypothalamic neurons (23–25), and augmentation or attenuation of central GLP-1 signaling can exert profound effects on peripheral glucose metabolism (26, 27). Furthermore, intraportal but not systemic administration of a GLP-1R antagonist or ganglionic blockade impairs GLP-1R–dependent control of glucose clearance (28, 29). Taken together, these findings challenge conventional concepts that GLP-1 acts predominantly on islet β cells to control glucose homeostasis (20).

To elucidate the importance of islet GLP-1Rs for glucoregulation, we used a transgenic rescue strategy to selectively restore human GLP-1R expression in pancreatic ductal and β cells of *Glp1r*$^{-/-}$ mice. Islets isolated from *Glp1r*$^{-/-}$ mice that expressed the human GLP-1R in islets and pancreatic ductal cells (Pdx1-hGLP1R:*Glp1r*$^{-/-}$ mice) displayed functional coupling of GLP-1R agonism to the stimulation of insulin secretion. Pdx1-hGLP1R:*Glp1r*$^{-/-}$ mice exhibited restoration of the glucoregulatory, proliferative, and insulin stimulatory effects of the GLP-1R agonist exendin-4 (Ex-4) in vivo. Furthermore, Pdx1-hGLP1R:*Glp1r*$^{-/-}$ mice displayed improved glucose tolerance compared with that of *Glp1r*$^{-/-}$ mice. Hence, selective restoration of the GLP-1R in the murine pancreas reveals the essential physiological role of the islet GLP-1R in the regulation of β cell function and glucose homeostasis.

Results

Pancreatic GLP-1R expression in Pdx1-hGLP1R:Glp1r$^{-/-}$ *mice*. A 4.6-kb genomic sequence containing the 5′ promoter region of the mouse pancreatic and duodenal homeobox 1 (*Pdx1*) gene (30) was used to direct expression of the human GLP-1R cDNA (Pdx1-hGLP1R) in transgenic mice (Figure 1A). To selectively restore GLP-1R expression in pancreatic ductal and β cells, *Glp1r*$^{-/-}$ mice were crossed with Pdx1-hGLP1R transgenic mice, and the resulting Pdx1-hGLP1R:*Glp1r*$^{+/-}$ and *Glp1r*$^{+/-}$ mice were crossed to generate Pdx1-hGLP1R:*Glp1r*$^{-/-}$ mice. WT littermates (*Glp1r*$^{+/+}$ mice) and Pdx1-hGLP1R and *Glp1r*$^{-/-}$ mice were used as controls (Figure 1B).

Real-time PCR demonstrated expression of the transgene in Pdx1-hGLP1R:*Glp1r*$^{-/-}$ mice predominantly in pancreatic islets

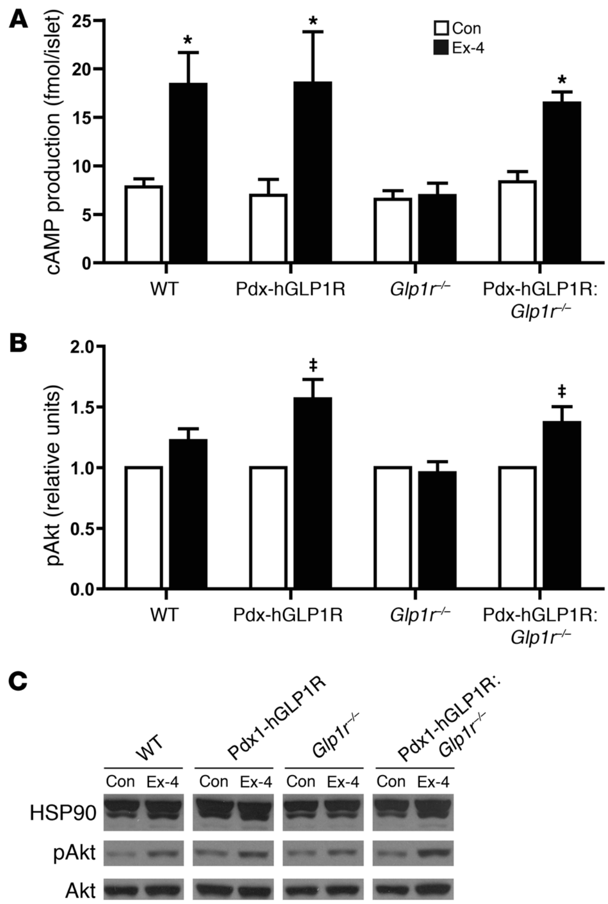

Figure 2
Restoration of islet GLP-1R signaling in islets from Pdx1-hGLP1R:*Glp1r*$^{-/-}$ mice. GLP-1R signaling pathways were assessed ex vivo in islets isolated from Pdx1-hGLP1R:*Glp1r*$^{-/-}$ and control mice. (**A**) Total cAMP accumulation in islets (n = 6–9) incubated for 15 minutes in media containing 10 nM Ex-4 compared with those incubated in control media (Con). (**B** and **C**) Phosphorylated Akt levels were assessed by Western blot of protein lysates from islets that were incubated for 60 minutes in either control media or media containing 10 nM Ex-4. (**B**) Quantification of pAkt levels was performed on densitometry data from 3 to 8 independent experiments for each genotype. (**C**) A representative blot is shown. HSP90 was used as a loading control. *P < 0.05 versus control; ‡P < 0.05 versus Ex-4–treated *Glp1r*$^{-/-}$ islets.

(Figure 1, D and E). Moreover, the relative levels of human *GLP1R* mRNA transcripts in Pdx1-hGLP:*Glp1r*$^{-/-}$ mouse islets were similar to levels of endogenous murine *Glp1r* mRNA transcripts in islets from WT control mice (Figure 1, D and E). Immunohistochemistry localized the human GLP-1R (hGLP-1R) protein to pancreatic islets and occasional ductal cells in histological sections from Pdx1-hGLP1R:*Glp1r*$^{-/-}$ pancreata (Figure 1C). The expression of the hGLP1R transgene did not significantly alter the basal levels of mRNA transcripts encoding GLP-1–regulated genes important for glucose homeostasis (*Pdx1*, *Ins2*, *Gipr*, *Glut2*, *Gck*, *Kir6.2*, *Akt1*) in islets from Pdx1-hGLP1R:*Glp1r*$^{-/-}$ mice (Supplemental Figure 1; supplemental material available online with this article; doi:10.1172/JCI42497DS1). Two independent lines of transgenic Pdx1-hGLP1R:*Glp1r*$^{-/-}$ mice were generated and analyzed. Both lines showed similar patterns of transgene expression and metabolic (glucose tolerance, insulin secretion, and food intake) responses to GLP-1R agonists (data not shown); therefore, all of the results presented herein are derived from analysis of a single transgenic mouse line.

Restoration of a functional GLP-1R in pancreatic islets of Pdx1-hGLP1R:Glp1r$^{-/-}$ mice. Engagement of the GLP-1R activates intracellular signaling cascades, leading to enhanced glucose-stimulated insulin secretion from pancreatic islets (31). The GLP-1R agonist Ex-4 significantly increased levels of cAMP in isolated islets from WT and Pdx1-hGLP1R transgenic mice but not in *Glp1r*$^{-/-}$ islets (Figure 2A); islets from Pdx1-hGLP1R:*Glp1r*$^{-/-}$ mice exhibited restoration of Ex-4–dependent stimulation of cAMP accumulation (Figure 2A). Consistent with these findings, Ex-4 promoted Akt phosphorylation in Pdx1-hGLP1R:*Glp1r*$^{-/-}$ transgenic islets (Figure 2, B and C). Hence, the human GLP-1R is functional and engages downstream signal transduction pathways in Pdx1-hGLP1R:*Glp1r*$^{-/-}$ islets.

We next examined whether restoration of GLP-1R signaling in Pdx1-hGLP1R:*Glp1r*$^{-/-}$ islets was coupled to GLP-1–stimulated enhancement of insulin secretion. Perifusion of isolated islets ex vivo with 16.7 mM glucose induced insulin secretion to similar levels as those from islets of all genotypes (Figure 3, A and B). When GLP-1 was added to the 16.7 mM glucose perifusion media, both WT and Pdx1-hGLP1R transgenic islets responded with a sustained increase in insulin secretion (Figure 3C). In comparison, islets from *Glp1r*$^{-/-}$ mice did not increase insulin secretion in response to GLP-1 (Figure 3, C and D). Expression of the hGLP1R transgene in Pdx1-hGLP1R:*Glp1r*$^{-/-}$ islets restored the direct potentiating effect of GLP-1 on glucose-stimulated insulin secretion (Figure 3, C and D).

Normalization of glucose tolerance in Pdx1-hGLP1R:Glp1r$^{-/-}$ mice. The observation that *Glp1r*$^{-/-}$ mice exhibit impaired glucose tolerance illustrates the importance of basal GLP-1R signaling for glucose homeostasis (32). We examined whether restoration of islet hGLP1R expression is sufficient for normalization of glucose tolerance in *Glp1r*$^{-/-}$ mice. Consistent with our original observations (33), the response to oral glucose was impaired in both male (Figure 4, A and C) and female (Figure 4, B and D) *Glp1r*$^{-/-}$ mice, without detectable changes in plasma insulin levels (Figure 4, E and F), as demonstrated previously (34–36). Plasma GLP-1 levels

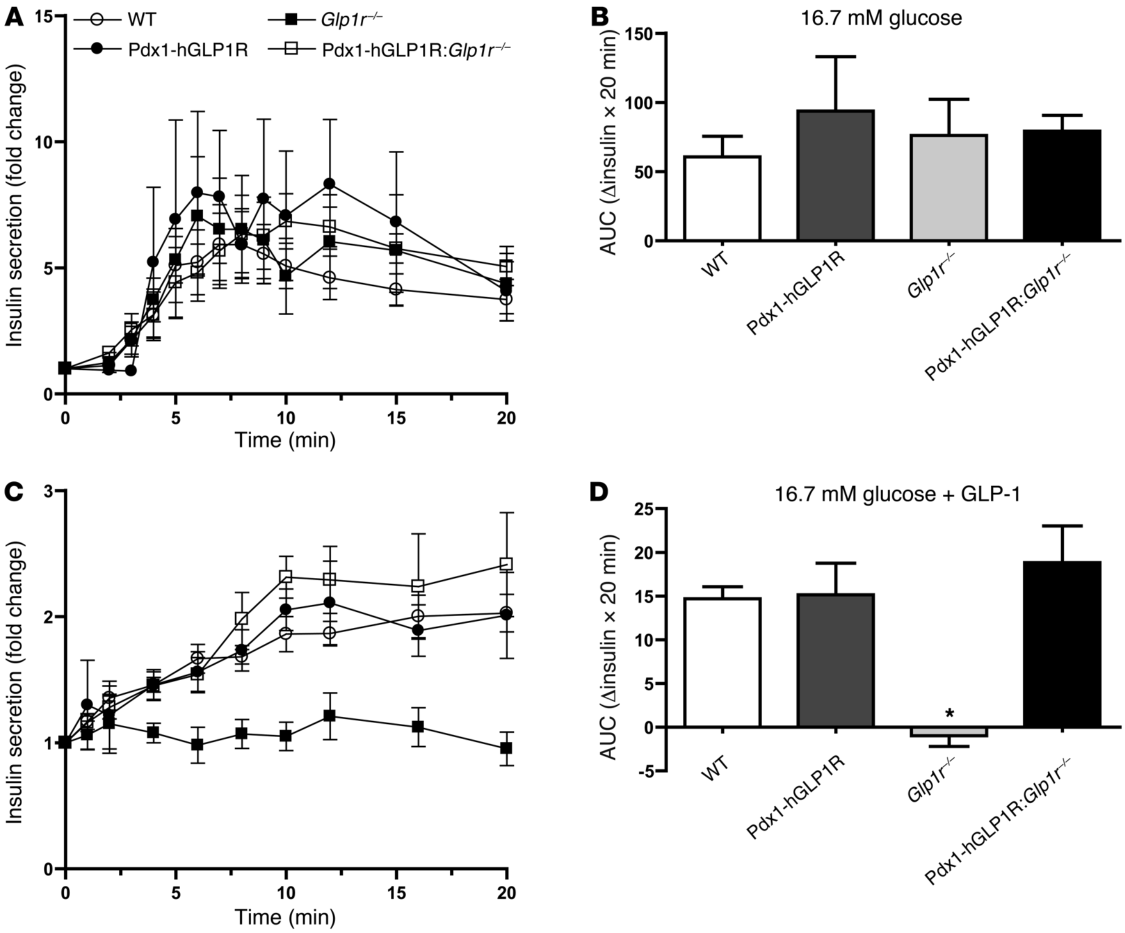

Figure 3

The effect of GLP-1 on glucose-stimulated insulin secretion is restored in Pdx1-hGLP1R:*Glp1r*$^{-/-}$ islets. Insulin secretion was assessed in isolated islets that were perifused with a Krebs-Ringer buffer that initially contained low glucose (2.8 mM), followed by high glucose (16.7 mM), and then by high glucose plus GLP-1 (10 nM). (**A**) The insulin secretory response to high glucose is presented as a fold change from the low-glucose condition, and (**C**) the response to the addition of GLP-1 is presented as a fold change from the high-glucose condition. Differences in the insulin secretory response stimulated by (**B**) high glucose and (**D**) high glucose plus GLP-1 were quantified by analysis of the incremental AUC for the change in insulin secretion over the 20-minute time period. n = 3–6. *$P < 0.05$ versus WT.

were increased in *Glp1r*$^{-/-}$ mice, but no changes in GIP or glucagon levels were detected across genotypes (Supplemental Figure 2, A–C). Remarkably, glucose tolerance was normalized in Pdx1-hGLP1R:*Glp1r*$^{-/-}$ mice (Figure 4, C and D). These results illustrate that basal β cell GLP-1R expression is important for maintaining glucose tolerance, independent of any potential compensatory adaptation arising from changes in levels of related glucoregulatory hormones such as glucagon or GIP.

Pharmacological activation of the pancreatic GLP-1R improves glucose tolerance. To determine the importance of the islet GLP-1R for the acute glucoregulatory response to exogenous GLP-1R agonists, we assessed glucose tolerance in the presence or absence of the GLP-1R agonist Ex-4. To avoid potential confounding influences of related endogenous incretin-like signals generated in response to enteral glucose (34), we first carried out i.p. glucose tolerance tests (IPGTTs). Ex-4 markedly reduced blood glucose and increased plasma insulin levels after i.p. glucose administration in WT mice (Figure 5A) and in Pdx1-hGLP1R transgenic mice (Figure 5B). In contrast, Ex-4 had no effect on i.p. glucose tolerance or insulin levels in *Glp1r*$^{-/-}$ mice (Figure 5C). A robust glucoregulatory and insulinotropic response to Ex-4 was restored in Pdx1-hGLP1R:*Glp1r*$^{-/-}$ mice, with the magnitude of the responses comparable to those observed in WT mice (compare Figure 5D with Figure 5A). Analogous results were seen after Ex-4 administration, in conjunction with oral glucose administration (Supplemental Figure 3). Hence, selective GLP-1R activation in pancreatic islets is sufficient to convey a robust pharmacodynamic response coupled to improvements in glucose homeostasis.

Absence of extrapancreatic metabolic effects of Ex-4 in Pdx1-hGLP1R:Glp1r$^{-/-}$ *mice*. As GLP-1R activation may also regulate glucose homeostasis through actions on the gastrointestinal tract and CNS (20), extrapancreatic GLP-1R actions might confound interpretation of data obtained in Pdx1-hGLP1R:*Glp1r*$^{-/-}$ mice. Accordingly, we assessed whether Ex-4 inhibited gastric emptying in mice of different genotypes. Ex-4 reduced the rate of appearance of acetaminophen in plasma from WT and Pdx1-hGLP1R transgenic mice (Figure 6, A and B) but had no effect on gastric emptying in *Glp1r*$^{-/-}$ mice (Figure 6C) or in Pdx1-hGLP1R:*Glp1r*$^{-/-}$ mice

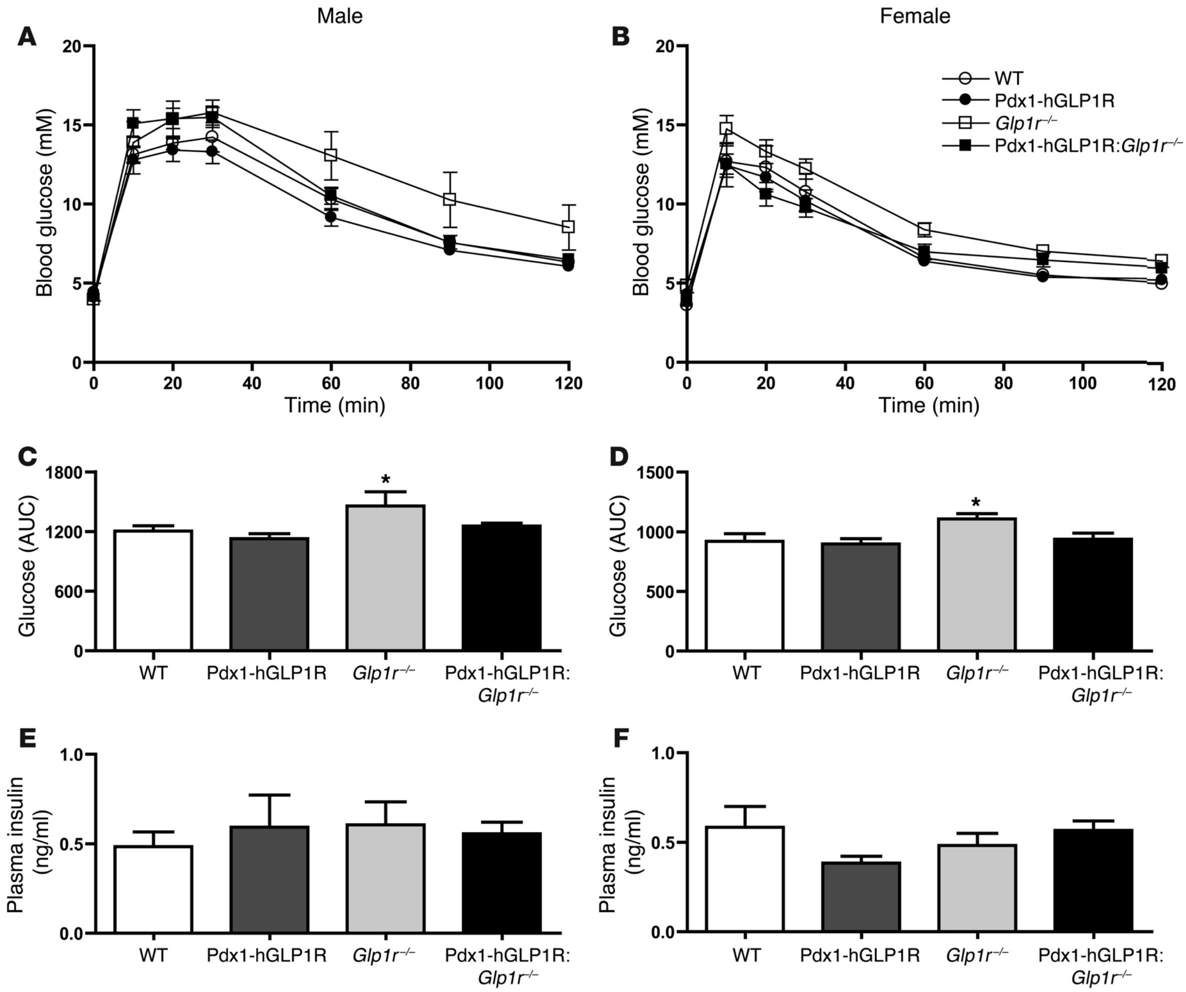

Figure 4

Normal glucose tolerance is restored in Pdx1-hGLP1R:*Glp1r*$^{-/-}$ mice. The response to an oral glucose challenge (OGTT; 1.5 g/kg of body weight) in (**A**) male and (**B**) female Pdx1-hGLP1R:*Glp1r*$^{-/-}$ mice was compared with that of WT, Pdx1-hGLP1R, and *Glp1r*$^{-/-}$ mice. Differences in the glucose excursion between genotypes for both (**C**) male and (**D**) female mice were quantified by comparing total AUC for glucose from 0 to 120 minutes. Plasma insulin levels in (**E**) male and (**F**) female mice were measured in samples collected 10 minutes after glucose administration. n = 6–11. *P < 0.05 versus WT.

(Figure 6D). Similarly, Ex-4 significantly reduced food intake in WT (Figure 7A) and Pdx1-hGLP1R transgenic mice (Figure 7B) but not in *Glp1r*$^{-/-}$ mice (Figure 7C) or in Pdx1-hGLP1R:*Glp1r*$^{-/-}$ mice (Figure 7D). These findings provide evidence for disruption of classical GLP-1R–regulated circuits in the nervous system of Pdx1-hGLP1R:*Glp1r*$^{-/-}$ mice.

Peripherally or centrally administered GLP-1R agonists also promote neuronal activation, detected by analysis of *c-fos* expression in the hindbrain and hypothalamus (15, 37, 38). Hence, we assessed whether Ex-4 administered via i.p. injection induced *c-fos* expression in the brains of Pdx1-hGLP1R:*Glp1r*$^{-/-}$ mice. Ex-4 increased levels of *c-fos* mRNA transcripts in the area postrema (AP) and nucleus of the solitary tract (NTS) areas of the hindbrain (Figure 8, A and B) in WT and Pdx1-hGLP1R mice but not in *Glp1r*$^{-/-}$ or Pdx1-hGLP1R:*Glp1r*$^{-/-}$ mice (Figure 8, A and B). The number of c-Fos–positive neurons in the AP and NTS was robustly increased by Ex-4 treatment in WT and Pdx1-hGLP-1R mice (Figure 8, C–E); however, these effects were completely absent in *Glp1r*$^{-/-}$ mice and substantially diminished or absent in Pdx1-hGLP1R:*Glp1r*$^{-/-}$ mice (Figure 8, C–E). Taken together, these findings further illustrate disruption of central GLP-1R signaling in Pdx1-hGLP1R:*Glp1r*$^{-/-}$ mice.

The extrapancreatic effects of the GLP-1R antagonist exendin$^{(9–39)}$ *are absent in Pdx1-hGLP1R:Glp1r*$^{-/-}$ *mice.* As pharmacological inhibition of brain GLP-1R signaling impairs glucose tolerance (27), we sought complementary evidence that the brain GLP-1R system was not functional in Pdx1-hGLP1R:*Glp1r*$^{-/-}$ mice. Accordingly, we assessed the effect of i.c.v. administration of the GLP-1R antagonist exendin$^{(9–39)}$ (Ex-9) on glucose tolerance. Consistent with previous findings (27), i.c.v. Ex-9 impaired glucose tolerance in WT (Figure 9A) and Pdx1-hGLP1R mice (Figure 9B). However, i.c.v. Ex-9 had no effect on glucose tolerance in *Glp1r*$^{-/-}$ mice (Figure 9C) or in Pdx1-hGLP1R:*Glp1r*$^{-/-}$ mice (Figure 9D). Taken together, these findings demonstrate absence of GLP-1R signaling in CNS neurons functionally coupled to regulation of glucose homeostasis in Pdx1-hGLP1R:*Glp1r*$^{-/-}$ mice. Intriguingly, the ability of peripheral Ex-9 to impair i.p. glucose tolerance in WT and Pdx1-hGLP1R mice (Figure

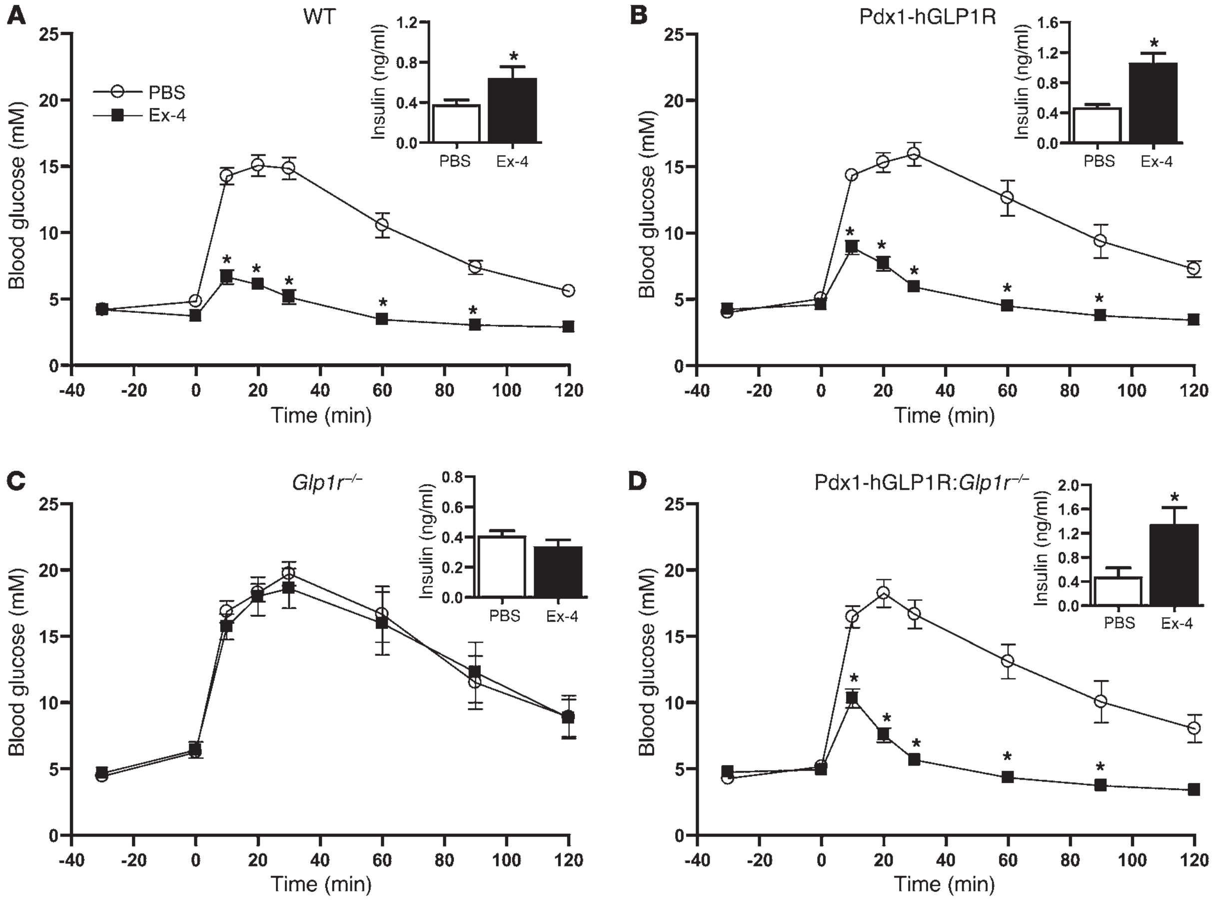

Figure 5

The effect of Ex-4 on glucose tolerance is restored in Pdx1-hGLP1R:*Glp1r*$^{-/-}$ mice. The response to an i.p. glucose challenge (IPGTT; 1.5 g/kg of body weight) in fasted male mice was assessed 30 minutes after an i.p. injection of either vehicle (PBS) or Ex-4 (1 μg). Blood glucose levels in (**A**) WT, (**B**) Pdx1-hGLP1R, (**C**) *Glp1r*$^{-/-}$, and (**D**) Pdx1-hGLP1R:*Glp1r*$^{-/-}$ mice were monitored throughout the experiment. Plasma insulin levels (insets) were measured in samples collected 10 minutes after glucose administration. n = 5–11. *P < 0.05 versus PBS.

10, A and B) was absent not only in *Glp1r*$^{-/-}$ mice (Figure 10C) but also in Pdx1-hGLP1R:*Glp1r*$^{-/-}$ mice (Figure 10D). These unexpected findings imply that the actions of Ex-9 to impair glucose tolerance are dependent in part on central GLP-1R signaling.

Pharmacological activation of the β *cell GLP-1R promotes expansion of* β *cell mass but does not increase pancreatic weight*. In young rodents for which the capacity for cellular growth and proliferation is relatively high, GLP-1R agonists stimulate β cell proliferation and promote expansion of β cell mass (39, 40). To assess whether GLP-1R–dependent expansion of β cell mass represents a direct effect mediated by the islet GLP-1R, we treated 8- to 12-week-old high-fat fed mice with Ex-4 for 10 days. Ex-4 produced a significant increase in β cell mass (Figure 11A) and proliferation (Figure 11, B and C) in Pdx1-hGLP1R:*Glp1r*$^{-/-}$ mice. In WT and Pdx1-hGLP1R mice, this identical treatment regimen did not affect β cell mass (Figure 11A) or proliferation (Figure 11, B and C), likely due to the 10% reduction in body weight observed in WT and Pdx1-hGLP1R mice but not Pdx1-hGLP1R:*Glp1r*$^{-/-}$ mice after Ex-4 administration.

As GLP-1R agonists also increase the mass of the entire pancreas (18, 41) and small bowel (42), we examined whether these trophic effects were mediated indirectly through the β cell GLP-1R. Consistent with previous findings (39, 43), a 10-day course of Ex-4 administration in older mice did not increase β cell mass (Figure 12A) but significantly increased the mass of the pancreas (Figure 12B) and small bowel (Figure 12C) in WT and Pdx-1-hGLP-1R transgenic mice. In contrast, no significant changes in pancreatic or small bowel mass were detected in *Glp1r*$^{-/-}$ or Pdx1-hGLP1R:*Glp1r*$^{-/-}$ mice (Figure 12, B and C). Ex-4 treatment also increased levels of *Irs2*, *Gck*, and *Ins2* mRNA transcripts in the pancreata of Pdx1-hGLP1R:*Glp1r*$^{-/-}$ mice (Figure 12, D–F). However, Ex-4 had no effect on expression of *Egfr*, *Pap*, and *Reg3a* mRNA transcripts, consistent with the predominant exocrine localization of these mRNAs in the pancreas (Figure 12, G–I). These results indicate that selective restoration of the β cell GLP-1R is not sufficient to transmit a GLP-1R–dependent growth-promoting signal to the exocrine pancreas or small bowel.

Discussion

The incretin concept describes the potentiation of glucose-stimulated insulin secretion after enteral glucose ingestion by gut-derived factors, predominantly GIP and GLP-1. Nevertheless, the widespread distribution of GLP-1R expression in extrapancreatic sites, such as the brain and peripheral nerves (29, 44, 45), illustrates that the glucoregulatory actions of GLP-1 are complex and

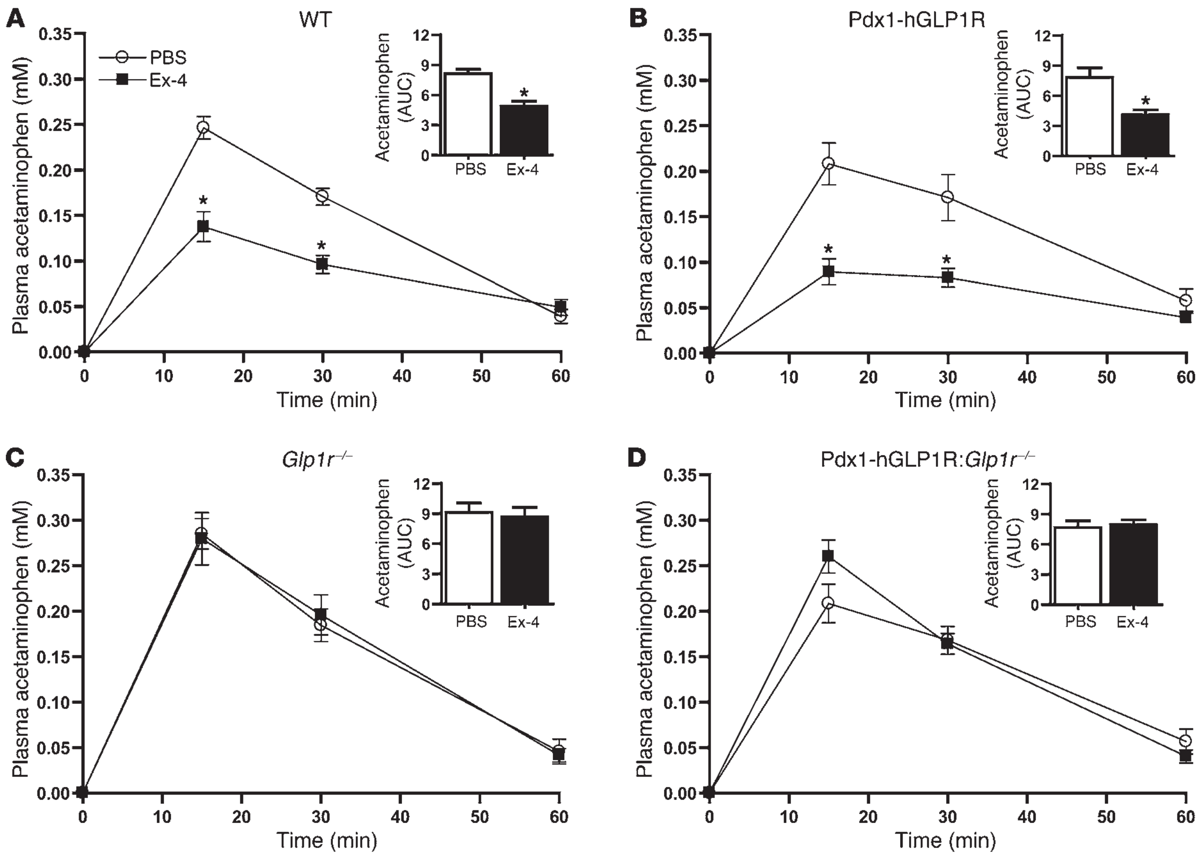

Figure 6
The effect of Ex-4 on gastric emptying is absent in Pdx1-hGLP1R:*Glp1r*$^{-/-}$ mice. After a 6-hour fast, male mice were injected with either vehicle (PBS) or Ex-4, 30 minutes prior to an oral gavage of glucose (1.5 g/kg) and acetaminophen (0.1 g/kg). The appearance of acetaminophen in plasma samples was used as a measure of gastric emptying in (**A**) WT, (**B**) Pdx1-hGLP1R, (**C**) *Glp1r*$^{-/-}$, and (**D**) Pdx1-hGLP1R:*Glp1r*$^{-/-}$ mice. Differences in acetaminophen absorption were quantified by comparing the total AUC for plasma acetaminophen from 0 to 60 minutes (insets). n = 5–12. *P < 0.05 versus PBS.

involve multiple tissues beyond the β cell. Moreover, a combination of gain- and loss-of-function studies support the importance of peripheral GLP-1–regulated neural circuits as mediators of glucose homeostasis. For example, activation of GLP-1R signaling in the portal vein leads to enhanced glucose clearance without changes in levels of plasma insulin (21, 46, 47). Conversely, selective interruption of portal GLP-1R signaling using antagonists impairs glucose clearance (21, 29). Hence, the available evidence invokes a role for peripheral GLP-1R–dependent control of glucose homeostasis, independent of changes in islet hormones (48).

The observations that the proglucagon gene is expressed in the CNS (24, 49) and that proglucagon-derived peptides, including GLP-1, are widely distributed to multiple CNS neurons that also express the GLP-1R (25, 50) raised the possibility that central GLP-1R signaling controls pathways important for metabolic homeostasis. Activation of central GLP-1Rs regulates food intake (16), interoceptive stress (51), blood pressure (38), and adipocyte lipid storage (52). Moreover, CNS GLP-1Rs also control peripheral insulin sensitivity and muscle glycogen synthesis (7, 53), and central GLP-1R blockade increased glycemic excursion after i.p. glucose challenge in rats (27).

The potential glucoregulatory signals arising from GLP-1Rs in multiple tissues bring into question the relative importance of the pancreatic GLP-1R for control of glucose homeostasis. As tissue-specific disruption of the *Glp1r* gene in key tissues has not yet been described, we used a transgenic strategy for selective restoration of GLP-1R expression in ductal and islet cells in the pancreas of *Glp1r*$^{-/-}$ mice. The observations that food intake and gastric emptying were insensitive to exogenous GLP-1R activation provide important evidence for disruption of classical GLP-1R–dependent CNS pathways in Pdx1-hGLP1R:*Glp1r*$^{-/-}$ mice. Furthermore, the failure of peripheral Ex-4 to activate c-fos expression, coupled with the inability of i.c.v. Ex-9 to cause deterioration in glucose tolerance, further supports the functional disruption of CNS GLP-1R circuits in Pdx1-hGLP1R:*Glp1r*$^{-/-}$ mice. Hence, the available evidence supports the use of Pdx1-hGLP1R:*Glp1r*$^{-/-}$ mice as a suitable model for analysis of the importance of both endogenous and pharmacological pancreatic GLP-1R activation for control of glucose homeostasis.

Nevertheless, it is important to acknowledge certain caveats in the interpretation of data obtained using Pdx1-hGLP1R:*Glp1r*$^{-/-}$ mice. First, it is impossible to rule out a small contribution to regulation of glucose homeostasis from one or more extrapancreatic sites, despite lack of evidence supporting the existence of functional CNS GLP-1Rs. Theoretically, *Glp1r*$^{-/-}$ mice may have evolved compensatory mechanisms leading to selective downregulation of extrapancreatic glucoregulatory mechanisms, making

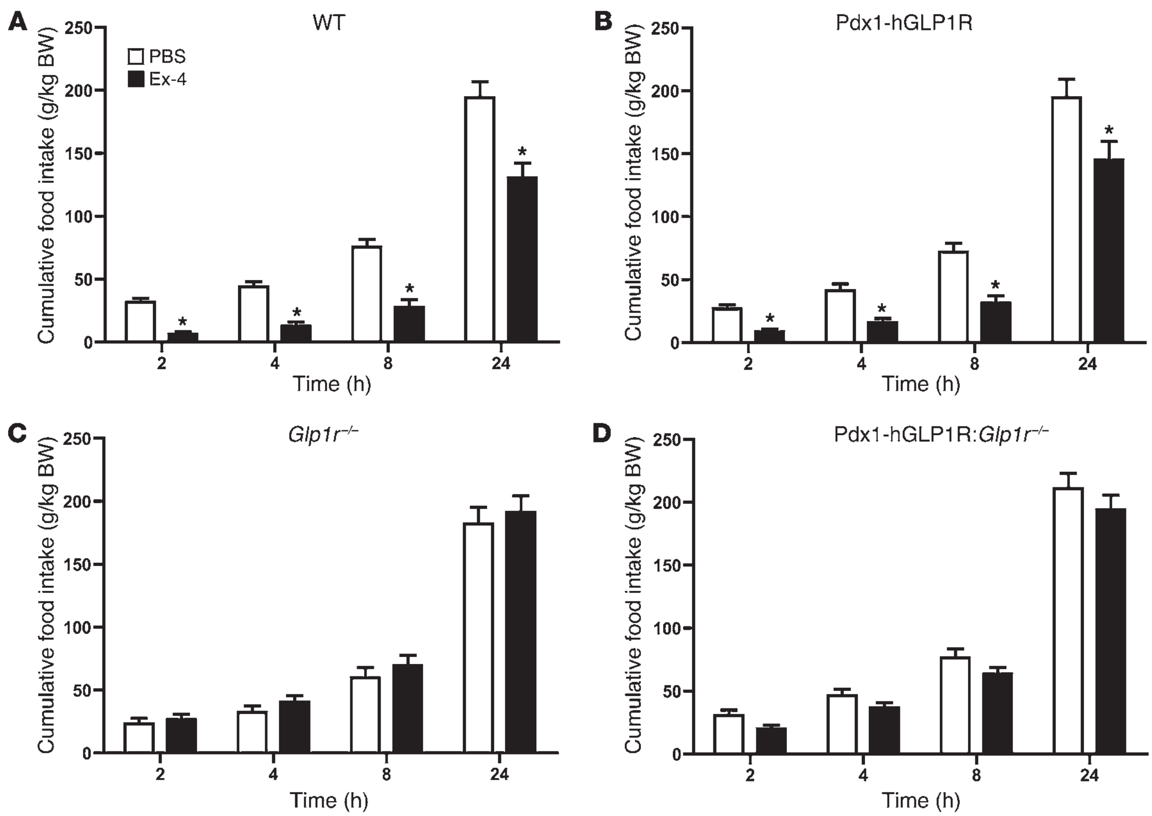

Figure 7
The effect of Ex-4 on food intake is absent in Pdx1-hGLP1R:*Glp1r*$^{-/-}$ mice. Food intake in male mice, after an overnight fast, was assessed after injection of either vehicle (PBS) or Ex-4. Cumulative food intake upon refeeding was recorded at 2, 4, 8, and 24 hours in (**A**) WT, (**B**) Pdx1-hGLP1R, (**C**) *Glp1r*$^{-/-}$, and (**D**) Pdx1-hGLP1R:*Glp1r*$^{-/-}$ mice. n = 7–11. *P < 0.05 versus PBS.

these actions more difficult to detect. We did not detect significant differences in islet expression of important GLP-1R–sensitive glucoregulatory genes, such as *Pdx1*, *Glut2*, *Gck*, *Kir6.2*, *Gipr*, or *Ins2*, in Pdx1-hGLP1R:*Glp1r*$^{-/-}$ mice (Supplemental Figure 1), and the islet response to exogenous Ex-4 was comparable to that in Pdx1-hGLP1R:*Glp1r*$^{-/-}$ mice (Figures 2 and 3). Nevertheless, we cannot completely eliminate the possibility that transgenic islets might exhibit enhanced coupling to downstream signaling pathways, leading to increased GLP-1R–dependent glucoregulatory activity arising from islet transgene expression.

Given the considerable evidence supporting a role for pharmacological levels of GLP-1 in the activation of insulin secretion and glucose homeostasis (54), it is perhaps not unexpected that restoration of islet GLP-1R expression was sufficient for restoring a robust glucoregulatory and insulinotropic response to exogenous Ex-4 in Pdx1-hGLP1R:*Glp1r*$^{-/-}$ mice. Similarly, GLP-1R activation leads to β cell proliferation in rodents in vivo (55) and in islet cells ex vivo (56); hence, it seems reasonable that restoration of islet GLP-1R expression restores GLP-1R–dependent stimulation of β cell proliferation and expansion of β cell mass. In contrast, Ex-4 was unable to increase the mass of the pancreas or small bowel in Pdx1-hGLP1R:*Glp1r*$^{-/-}$ mice, demonstrating that the trophic actions of GLP-1R agonists on these tissues require input from extrapancreatic GLP-1Rs. Unexpectedly, despite restoration of islet GLP-1R expression, the antagonist Ex-9 did not impair glucose homeostasis after i.p. glucose homeostasis in Pdx1-hGLP1R:*Glp1r*$^{-/-}$ mice. More surprisingly, restoration of basal levels of GLP-1R expression in *Glp1r*$^{-/-}$ islets was sufficient to normalize glucose tolerance in *Glp1r*$^{-/-}$ mice. The preferential improvement in i.p. tolerance compared with oral glucose tolerance in Pdx1-hGLP1R:*Glp1r*$^{-/-}$ mice is consistent with failure to restore the GLP-1R–dependent control of gastric emptying and in agreement with our original findings of increased fasting glucose and abnormal i.p. glucose tolerance in *Glp1r*$^{-/-}$ mice (33). These latter findings strongly suggest that the low basal levels of endogenous GLP-1, continuously secreted in the absence of nutrient ingestion, convey a physiologically important endocrine signal to islet GLP-1Rs. Taken together, the findings in Pdx1-hGLP1R:*Glp1r*$^{-/-}$ mice provide further support for an important role for islet GLP-1R signaling in the integrated GLP-1R–dependent control of glucose homeostasis (20). It seems likely that ongoing genetic studies elucidating the importance of enhanced versus disrupted GLP-1R signaling in the central and peripheral nervous system and pancreas will further refine our understanding of the complexity of incretin action.

Methods

Animal experiments. Transgenic mice were generated by pronuclear injection of a DNA construct containing the 5′ promoter sequence (4.6 kb) of the mouse *Pdx1* gene (30), the human GLP-1R cDNA (2.4 kb), and a poly-A signal (0.6 kb) into fertilized eggs. Mice that contained the Pdx1-hGLP1R transgene were backcrossed to the C57BL/6 inbred strain. Pdx1-hGLP1R transgenic mice were then crossed to *Glp1r*$^{-/-}$ mice (33) in the C57BL/6 background. To generate Pdx1-hGLP1R:*Glp1r*$^{-/-}$ mice and the littermate

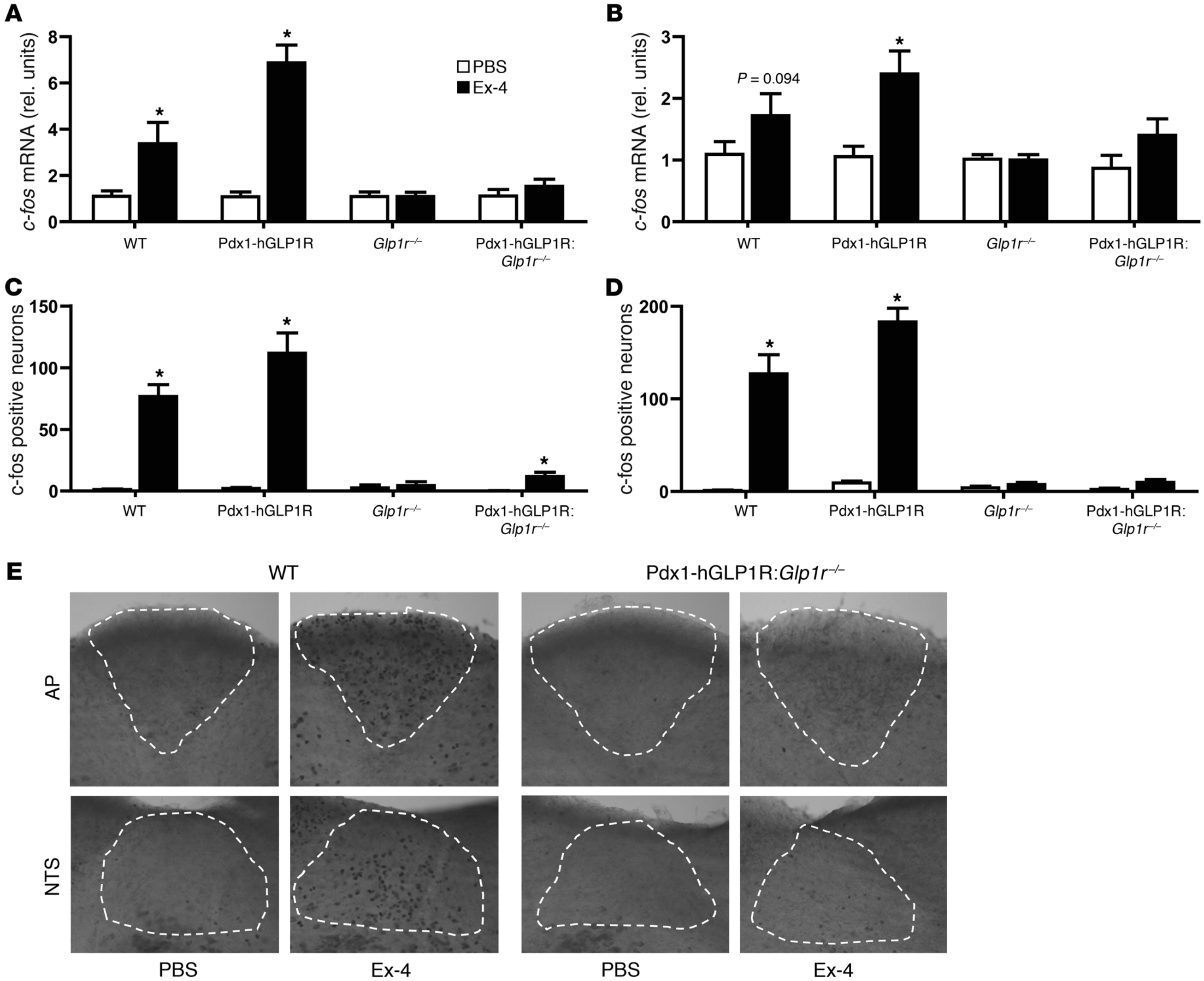

Figure 8

Hindbrain c-fos activation in response to peripheral Ex-4 is severely blunted in Pdx1-hGLP1R:*Glp1r*$^{-/-}$ mice. *c-fos* mRNA transcript levels after i.p. injection of Ex-4 (4 nmol/kg) or vehicle (PBS) in (**A**) the AP and (**B**) the NTS regions of the hindbrain in WT, Pdx1-hGLP1R, *Glp1r*$^{-/-}$, and Pdx1-hGLP1R:*Glp1r*$^{-/-}$ mice were determined by quantitative real-time PCR analysis. rel., relative. n = 5–8. $^{*}P < 0.05$ versus PBS. The number of neurons in (**C**) the AP and (**D**) the NTS that expressed c-Fos protein after i.p. injection of Ex-4 (10 nmol/kg) or PBS was determined via IHC analysis. n = 4–8. $^{*}P < 0.05$ versus PBS. (**E**) Representative images of the AP and the NTS stained for c-Fos. Dashed lines define the areas of the AP and the NTS. Original magnification, ×20.

controls used for all experiments, hemizygous transgenic mice (Pdx1-hGLP1R:*Glp1r*$^{+/-}$ mice) were crossed to *Glp1r*$^{+/-}$ mice. Mice of the different genotypes were born in the expected Mendelian ratios, with approximately 1 out of every 8 mice exhibiting the Pdx1-hGLP1R:*Glp1r*$^{-/-}$ genotype. Mice were genotyped using 2 separate PCRs: one specifically detected the human GLP-1R transgene (5′-TCAAGGTCAACGGCTTATTAG-3′ and 5′-TAACGTGTCCCTAGATGAACC-3′ generating a 481-bp fragment), and the other detected the presence of either the endogenous *Glp1r* WT allele (5′-TACACAATGGGGAGCCCCTA-3′ and 5′-AAGTCATGGGATGTGTCTGGA-3′ generating a 437-bp fragment) or the neo-containing *Glp1r* knockout allele (5′-CTTGGGTGGAGAGGCTATTC-3′ and 5′-AGGTGAGATGACAGGAGATC-3′ generating a 280-bp fragment). All mice were housed under specific pathogen–free conditions in microisolator cages and maintained on a 12-hour-light cycle, with free access to food and water.

To assess the effects of chronic GLP-1R activation, older chow-fed male mice (approximately 6 months old) or young male mice (8 to 12 weeks old) fed a high-fat diet for 4 weeks (45% kcal from fat; Research Diets) were injected twice daily with 1 μg Ex-4 (California Peptide Research) for 10 days. To assess the number of proliferating β cells, 5-bromo-2′-deoxyuridine (BrdU; Sigma-Aldrich) was administered daily (50 mg/kg) over the course of the treatment period. At the end of the treatment period, mice were euthanized by CO_2 inhalation, tissues were excised, and the weights of the pancreata and small intestines were recorded. Immunohistochemical (IHC) analysis of formalin-fixed pancreas sections was carried out as previously described (57). The primary antibodies used for IHC were a rabbit anti-human GLP-1R (Lifespan, LS-A1205), a guinea pig anti-insulin (Invitrogen, 18-0067), and a rat mAb to BrdU (Abcam, ab6326). The insulin- and BrdU antibody–stained sections were scanned using the Scanscope

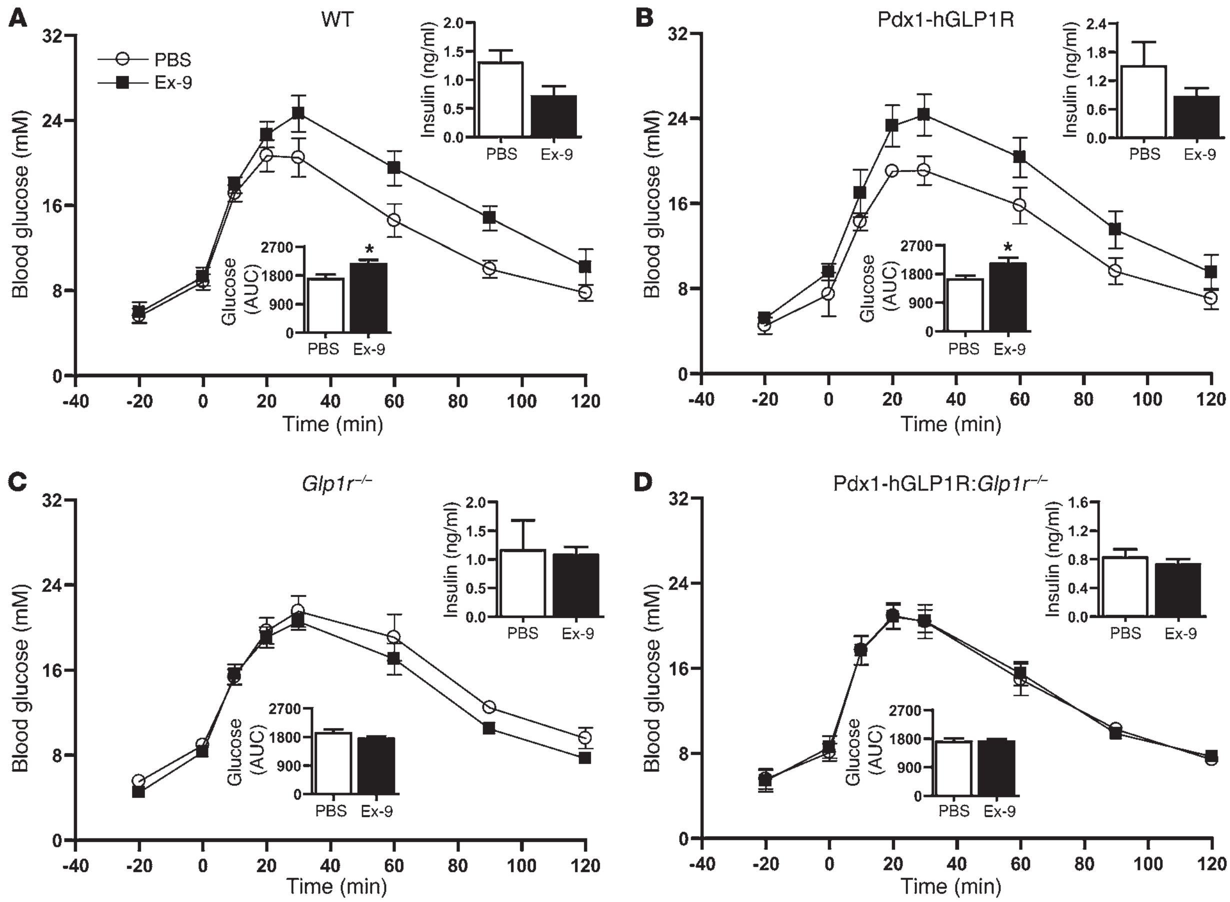

Figure 9

The effect of i.c.v Ex-9 on glucose tolerance is absent in Pdx1-hGLP1R:*Glp1r*$^{-/-}$ mice. The response to an i.p. glucose challenge (IPGTT; 1.5 g/kg of body weight) in fasted male mice was assessed 20 minutes after an i.c.v. injection of either vehicle (PBS) or Ex-9 (5 μg). Blood glucose levels in (**A**) WT, (**B**) Pdx1-hGLP1R, (**C**) *Glp1r*$^{-/-}$, and (**D**) Pdx1-hGLP1R:*Glp1r*$^{-/-}$ mice were monitored throughout the experiment. Differences in the blood glucose excursion in response to PBS compared with that for Ex-9 were quantified by comparing the total AUC (bottom insets) for glucose from 0 to 120 minutes. Plasma insulin levels (top insets) were measured in samples collected 10 minutes after glucose administration. *n* = 4–7. **P* < 0.05 versus PBS.

CS system (Aperio Technologies) at ×20 magnification. The digital images were analyzed with the Scanscope software (Aperio Technologies) using a preset positive pixel count algorithm to quantify the insulin-positive and insulin-negative areas. The number of BrdU$^+$ cells in islets was counted in serial sections. The β cell mass for each animal was calculated as the product of the total cross-sectional area of β cells divided by total pancreas area and the weight of the pancreas before fixation.

RNA preparation and quantitative real-time PCR. Total RNA was extracted from tissue samples using Tri Reagent (Sigma-Aldrich). For isolated islets and small brain samples, the RNeasy Mini Kit (Qiagen) was used. First-strand cDNA was synthesized from total RNA using the SuperScript III Synthesis System (Invitrogen) and random hexamers. Real-time quantitative PCR analysis was performed using TaqMan Gene Expression Assays and TaqMan Universal PCR Master Mix (Applied Biosystems) with the ABI Prism 7900 Sequence Detection System, according to the protocols provided by the manufacturer (Applied Biosystems). To determine the levels of expression of mouse and human *Glp1r* transcripts (Taqman assays Hs01006332_m1 and Mm01351008_m1) in various tissues, a standard curve quantification method was used (58), for which standard curves were generated with known amounts of cDNA for each gene assessed. For each tissue sample, the level of *Gapdh* (Taqman assay Mm03302249_g1) was used as an internal control. The relative levels of mRNA transcripts (*Pdx1*, *Ins2*, *Gipr*, *Glut2*, *Gck*, *Kir6.2*, *Akt1*, *Irs2*, *Egfr*, *Pap*, and *Reg3a*) in isolated islets or pancreas samples were quantified by the comparative Ct ($2^{-\Delta\Delta Ct}$) method (59), using either *Ppia* or *Iapp* as the internal control gene, as described previously (41, 60).

Islet experiments. After euthanasia via CO_2 inhalation, the pancreas was inflated via the pancreatic duct with collagenase type V (0.7 mg/ml) in HBSS, excised, and digested at 37°C for 10 to 15 minutes. The resulting digest was washed twice with cold HBSS (containing 0.25% w/v BSA), and islets were separated using a Histopaque density gradient (Sigma-Aldrich). The interface containing islets was removed and washed with HBSS containing BSA, and the islets were resuspended in RPMI containing 2 mM L-glutamine, 10 mM glucose, 1% BSA, 100 U/ml penicillin, and 100 μg/ml streptomycin. Islets were initially incubated at 37°C for 4 hours and were then handpicked into fresh RPMI with 5.6 mM glucose for overnight recovery (37°C, 5% CO_2). Prior to signaling experiments (cAMP measurement and Western blotting), islets were incubated in Krebs-Ringer bicarbonate buffer (KRB) containing 0.1% BSA, 10 mM HEPES (pH 7.4), and 2.8 mM glucose for 1 hour. Islets were then transferred into KRB containing 16.7 mM glucose with or without Ex-4 (10 nM). Batches of 40 islets were

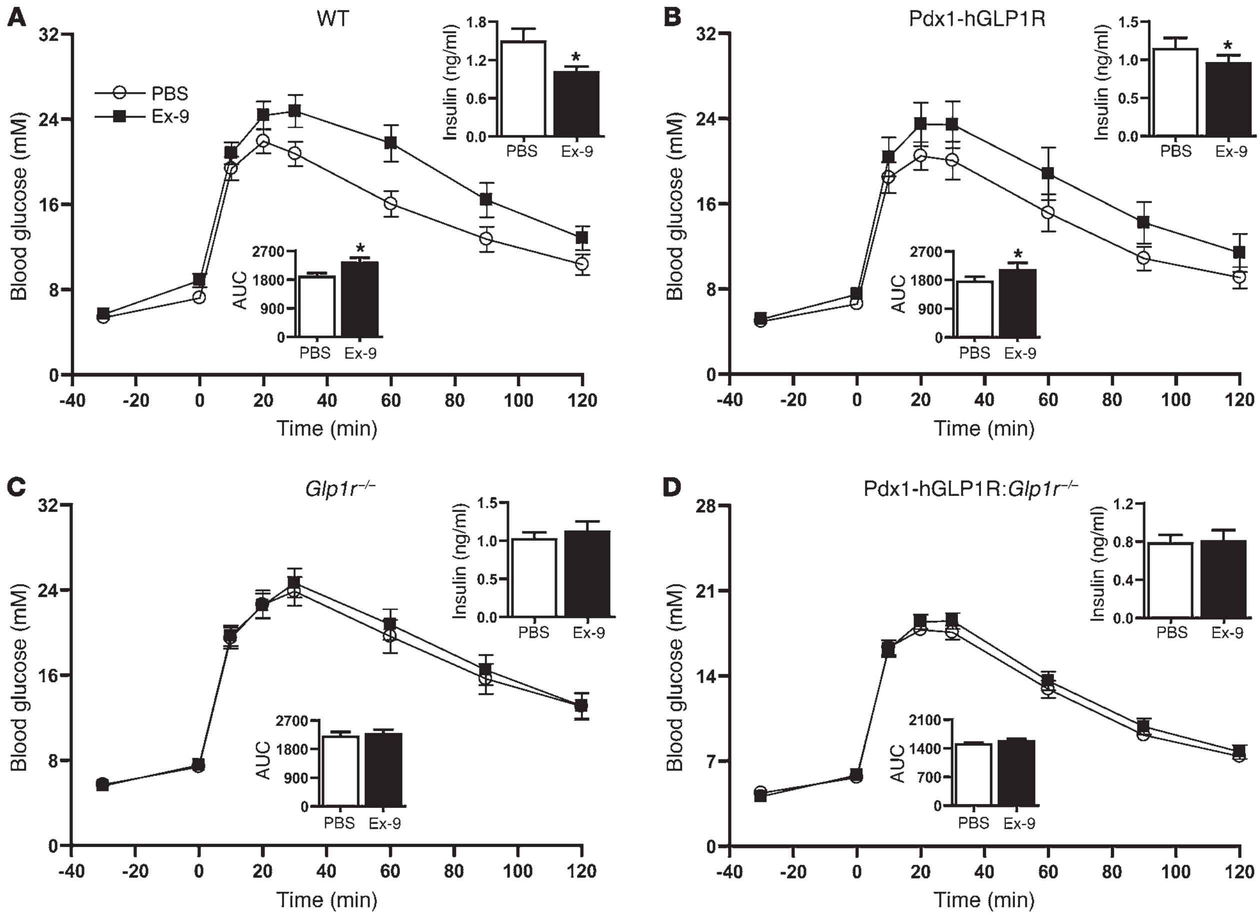

Figure 10
The effect of peripheral Ex-9 on glucose tolerance is absent in Pdx1-hGLP1R:*Glp1r*$^{-/-}$ mice. The response to an i.p. glucose challenge (IPGTT; 1.5 g/kg of body weight) in fasted male mice was assessed 30 minutes after an i.p. injection of either vehicle (PBS) or Ex-9 (5 μg). Blood glucose levels in (**A**) WT, (**B**) Pdx1-hGLP1R, (**C**) *Glp1r*$^{-/-}$, and (**D**) Pdx1-hGLP1R:*Glp1r*$^{-/-}$ mice were monitored throughout the experiment. Differences in the blood glucose excursion in response to PBS compared with that for Ex-9 were quantified by comparing the total AUC (bottom insets) for glucose from 0 to 120 minutes. Plasma insulin levels (top insets) were measured in samples collected 10 minutes after glucose administration. n = 12–20. *P < 0.05 versus PBS.

used for analysis of cAMP production. KRB was supplemented with 100 μM IBMX, and the experiment was terminated after 15 minutes by the addition of cold ethanol (at a final concentration of 65%). After sonication, total cAMP levels were measured using a cAMP RIA Kit (Biomedical Technologies). Batches of 80 islets were used to generate samples for assessing the levels of pAkt by Western blot. After 30 minutes of stimulation with glucose (16.7 mM) or glucose and Ex-4 (10 nM), islets were washed with cold PBS and resuspended in SDS sample buffer containing β-mercaptoethanol, boiled for 5 minutes, and stored at −20°C pending analysis.

For determination of glucose-stimulated insulin secretion, batches of 50 islets were placed in a perifusion chamber (capacity 1.3 ml) at 37°C and perifused at a flow rate of 1 ml/min, as described previously (61). Islets were first equilibrated for 30 minutes in KRB with 2.8 mM glucose. This was followed by perifusion with KRB containing 16.7 mM glucose for 30 minutes and followed by the addition of 10 mM GLP-1 (7–36) amide (Bachem) for a final 30 minutes. Fractions were collected at several time points, and insulin was measured using a rat insulin RIA Kit (Millipore). At the end of the experiment, islets were collected and lysed in acid ethanol for measurement of total insulin content. For each sample, the amount of insulin present was normalized to insulin content. The results from the high-glucose stimulation are presented as fold increase from basal (low glucose) conditions, and the results for the GLP-1 stimulation are presented as fold increase over high-glucose conditions.

Western blotting. Islet protein was separated by SDS-PAGE, transferred to nitrocellulose membranes, and blocked in either 5% BSA or 5% milk in TBS-T for 1 hour before incubation with primary antibodies overnight at 4°C. The primary antibodies for pAkt (Cell Signaling no. 9275) and Akt (Cell Signaling no. 9272) were diluted 1:1,000 in 5% BSA, and the antibody for HSP90 (BD Biosciences, no. 610418) was diluted 1:5,000 in 5% milk. Secondary antibodies were linked to horseradish peroxidase (GE Healthcare), and bands were visualized by exposure to BioMax film, (Kodak) using enhanced chemiluminescence (GE Healthcare). Densitometry was quantified using Scion Image software (Scion Corp).

Glucose tolerance tests. Glucose tolerance tests were carried out in 3- to 6-month-old male and female mice. After an overnight fast (16–18 hours), glucose (1.5 mg/g body weight) was administered via either an oral gavage (oral glucose tolerance test [OGTT]) or i.p. injection (IPGTT). In some experiments, Ex-4 (1 μg), Ex-9 (5 μg), or vehicle (PBS) was administered via i.p. injection 30 minutes prior to glucose administration. In a separate set of experiments, 5 μg Ex-9 or vehicle (PBS) was administered 20 min-

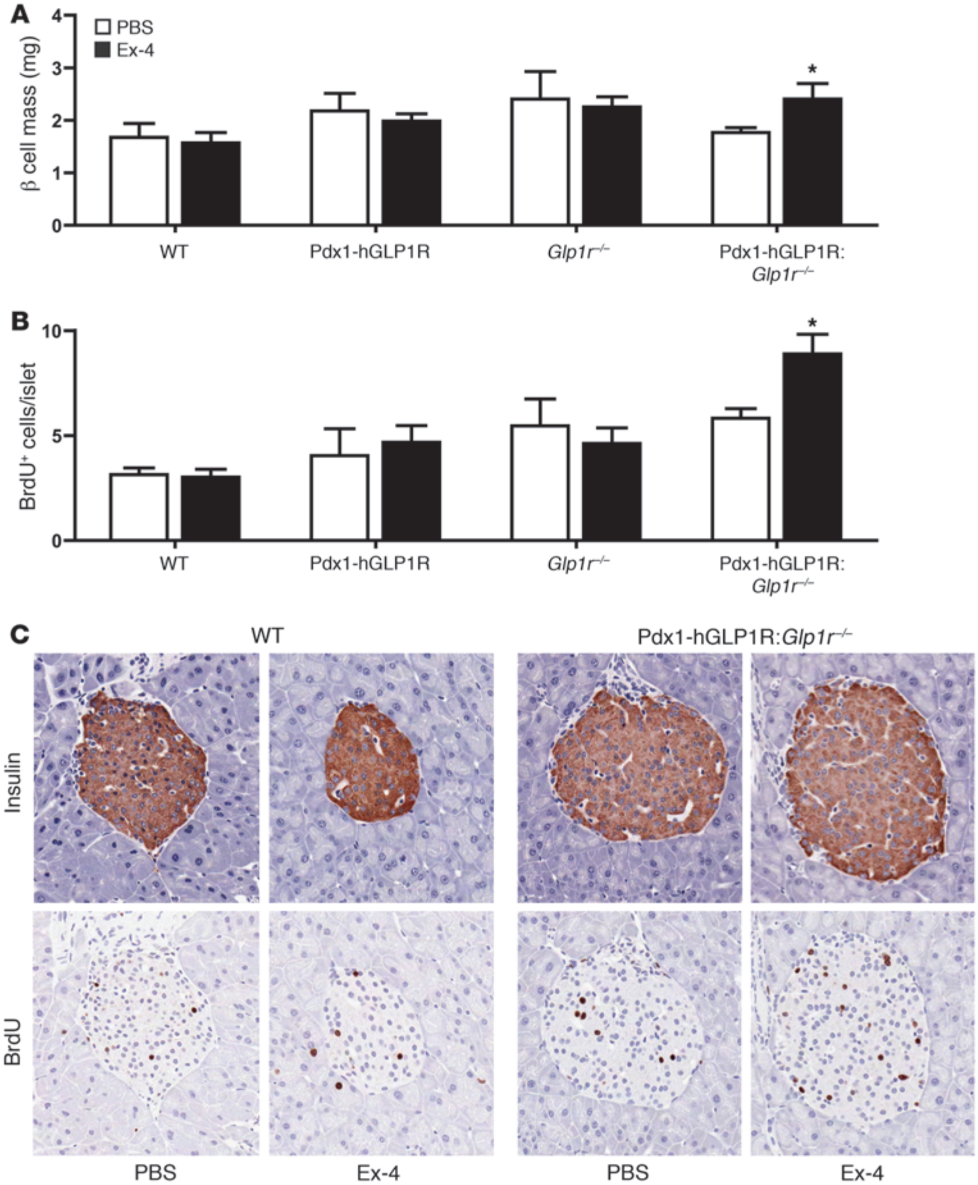

Figure 11

Ex-4 increases β cell mass and proliferation in Pdx1-hGLP1R:*Glp1r*$^{-/-}$ mice. After 10 days of Ex-4 (twice daily) or vehicle (PBS) injections (**A**) β cell mass and (**B**) the number of BrdU-positive islet cells were assessed via IHC analysis of pancreas sections from high-fat fed WT, Pdx1-hGLP1R, *Glp1r*$^{-/-}$, and Pdx1-hGLP1R:*Glp1r*$^{-/-}$ mice. n = 3–6. *P < 0.05 versus PBS. (**C**) Representative images of islets stained for insulin and BrdU. Original magnification, ×20.

utes prior to glucose by i.c.v. injection, as described previously (15). Blood samples were drawn from the tail vein immediately prior to any treatment and at 0, 10, 20, 30, 60, and 120 minutes after glucose loading. Blood glucose levels were measured using a Glucometer (Bayer). For plasma insulin, glucagon, GLP-1, and GIP determinations, blood samples (50 or 100 μl) were collected from the tail vein into EDTA-coated tubes 10 minutes after glucose loading, and plasma was separated by centrifugation at 4°C and stored at −20°C until assayed as described previously (62). Plasma insulin levels were measured using a mouse insulin ELISA Kit (Alpco) or a rat insulin RIA Kit (Millipore). Mice that were subject to i.c.v. injections were euthanized at the completion of the experiment. All other mice were allowed to recover for 1 week before repeating the glucose tolerance test with the alternative treatment.

Assessment of gastric emptying. In 4- to 5-month-old male mice that were fasted for 6 hours, the acetaminophen absorption test (63) was used to assess the rate of gastric emptying. Ex-4 (1 μg) or vehicle (PBS) was administered via i.p. injection 30 minutes prior to oral administration of a glucose solution that contained 1% (w/v) acetaminophen (Sigma-Aldrich). The dose of acetaminophen administered was 100 mg/kg. Tail vein blood (50 μl) was collected into EDTA-coated tubes at 0, 15, 30, and 60 minutes after acetaminophen administration. Plasma was separated by centrifugation at 4°C and stored at −20°C until measurement of acetaminophen levels using an enzymatic-spectrophotometric assay (Cambridge Life Sciences). All mice were allowed to recover for 1 week before the test was repeated with the alternative treatment.

Analysis of food intake. Mice fasted overnight (16–18 hours) were injected with either Ex-4 (1 μg) or vehicle (PBS) and then placed into individual cages containing preweighed rodent chow (Harlan Teklad no. 7012) (with free access to water). Food was weighed after 2, 4, 8, and 24 hours, and food intake was expressed as grams consumed per kilogram of body weight. All mice were allowed to recover for 1 week before the food intake measurements were repeated with the alternative treatment.

Assessment of c-FOS expression in the hindbrain. The number of c-FOS–immunoreactive neurons in specific brain regions after Ex-4 administration was assessed as described previously (64). Briefly mice were fasted for 3 hours prior to i.p. injection of either Ex-4 (10 nmol/kg) or vehicle (PBS). After

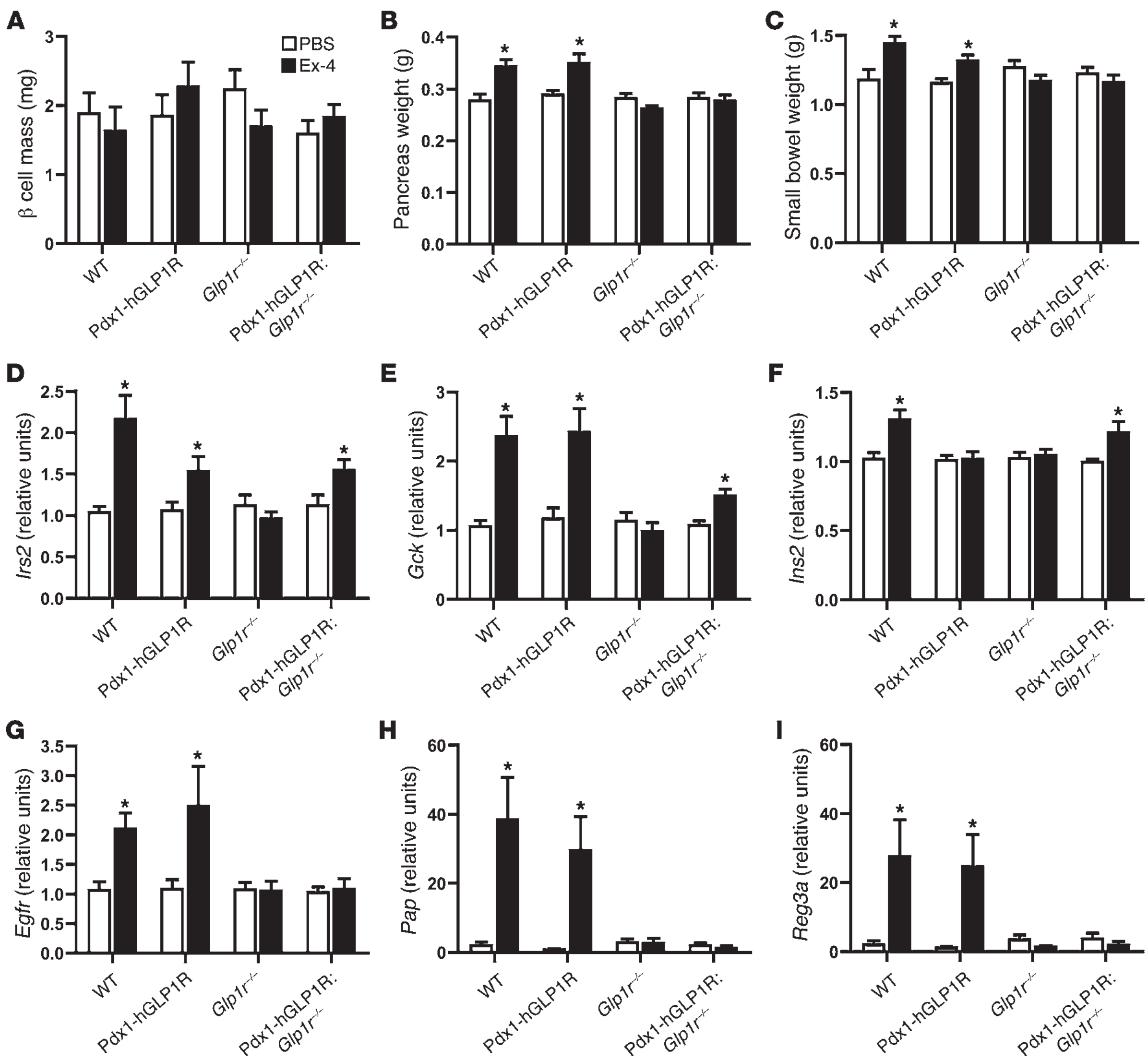

Figure 12
Effects of 10-day Ex-4 treatment (twice daily) on (**A**) β cell mass, (**B**) pancreatic weight, (**C**) small bowel weight, and (**D**–**I**) pancreatic gene expression in 6-month-old Pdx1-hGLP1R:*Glp1r*$^{-/-}$ and control mice. (**D**–**F**) The relative levels of genes involved in normal β cell function and (**G**–**I**) genes associated with the exocrine pancreas were quantified by real-time PCR analysis. n = 6–14. *P < 0.05 versus PBS.

60 minutes, mice were deeply anesthetized with avertin and transcardially perfused with ice-cold 4% paraformaldehyde. Whole brains were removed, post-fixed in 4% paraformaldehyde at 4°C for 24 hours, and then transferred to 10% sucrose solution before being frozen. Brains were stored at –80°C until 100-μm sections of the hindbrain were cut using a vibratome. Sections were processed for immunocytochemical detection of c-FOS using a conventional avidin-biotin-immunoperoxidase method (Standard Elite Vectastain ABC Kit, Vector Laboratories.). The anti-FOS antibody (Santa Cruz Biotechnology Inc., no. sc-52) was used at a dilution of 1:1,000. Brain sections corresponding to the level of the AP and the NTS were defined according to a mouse brain atlas (65). Using the Scion Image analysis software, the margins of the AP and NTS were defined using a dashed outline, and the number of FOS-positive neurons in that area were counted.

To assess *c-fos* mRNA levels in specific brain regions, Ex-4 (4 nmol/kg) was administered via i.p. injection 45 minutes prior to the dissection of the hindbrain. After decapitation, whole brains were rapidly removed and placed on a chilled stainless steel plate. A coronal cut was made just posterior of the obex, and another cut was made 1 mm anterior to this cut. The resulting section was placed on the stainless steel plate and the AP and NTS were dissected under magnification. RNA was extracted from these samples, and *c-fos* mRNA transcript levels were assessed using a Taqman Real-Time PCR gene expression assay (Applied Biosystems), with *Ppia* used as the internal control gene.

Statistics. All data are presented as mean ± SEM. The Prism software package (version 4; GraphPad) was used to complete the statistical analysis. Paired, 1-tailed *t* tests or 2-way ANOVA (with Bonferroni post-hoc analysis) were used to assess the differences in glucose tolerance, gastric emptying, and food intake data, where measurements were repeated on the same mice with each treatment. For all other data, unpaired, 1-tailed *t* tests or 1-way ANOVA (with Dunnett's multiple comparison test) were used to analyze differences among the control group and one or more independent treatment groups. A *P* value of less than 0.05 was considered significant.

Study approval. All procedures involving animals were conducted according to protocols and guidelines approved by the Toronto General Hospital, Mount Sinai Hospital, and Toronto Centre for Phenogenomics animal care committees.

Acknowledgments

D.J. Drucker is supported in part by a Canada Research Chair in Regulatory Peptides and a Banting and Best Diabetes Centre Novo Nordisk Chair in Incretin Biology. These studies were supported in part by CIHR operating grants MOP 82700 and the Merck Frosst Training Program in Incretin Biology (to D.J. Drucker) and MOP 86544 (to H.Y. Gaisano).

Received for publication September 2, 2011, and accepted in revised form November 2, 2011.

Address correspondence to: Daniel J. Drucker, Mount Sinai Hospital SLRI, 600 University Ave. TCP5-1004, Toronto, Ontario M5G 1X5, Canada. Phone: 416.361.2661; Fax: 416.361.2669; E-mail: d.drucker@utoronto.ca.

1. Cherrington AD. Banting Lecture 1997. Control of glucose uptake and release by the liver in vivo. *Diabetes*. 1999;48(5):1198–1214.
2. Sandoval D, Cota D, Seeley RJ. The integrative role of CNS fuel-sensing mechanisms in energy balance and glucose regulation. *Annu Rev Physiol*. 2008;70:513–535.
3. Ahima RS, Lazar MA. Adipokines and the peripheral and neural control of energy balance. *Mol Endocrinol*. 2008;22(5):1023–1031.
4. Scherer PE. Adipose tissue: from lipid storage compartment to endocrine organ. *Diabetes*. 2006; 55(6):1537–1545.
5. Lam TK, Gutierrez-Juarez R, Pocai A, Rossetti L. Regulation of blood glucose by hypothalamic pyruvate metabolism. *Science*. 2005;309(5736):943–947.
6. Lam TK, et al. Hypothalamic sensing of circulating fatty acids is required for glucose homeostasis. *Nat Med*. 2005;11(3):320–327.
7. Knauf C, et al. Role of central nervous system glucagon-like peptide-1 receptors in enteric glucose sensing. *Diabetes*. 2008;57(10):2603–2612.
8. Cheung GW, Kokorovic A, Lam CK, Chari M, Lam TK. Intestinal cholecystokinin controls glucose production through a neuronal network. *Cell Metab*. 2009;10(2):99–109.
9. Cummings DE, Overduin J. Gastrointestinal regulation of food intake. *J Clin Invest*. 2007;117(1):13–23.
10. Holst JJ, Gromada J. Role of incretin hormones in the regulation of insulin secretion in diabetic and nondiabetic humans. *Am J Physiol Endocrinol Metab*. 2004;287(2):E199–E206.
11. Nauck MA. Is glucagon-like peptide 1 an incretin hormone? *Diabetologia*. 1999;42(3):373–379.
12. Waget A, et al. Physiological and pharmacological mechanisms through which the DPP-4 inhibitor sitagliptin regulates glycemia in mice. *Endocrinology*. 2011;152(8):3018–3029.
13. Imeryuz N, Yegen BC, Bozkurt A, Coskun T, Villanueva-Pennacarrillo ML, Ulusoy NB. Glucagon-like peptide-1 inhibits gastric emptying via vagal afferent-mediated central mechanisms. *Am J Physiol*. 1997; 273(4 pt 1):G920–G927.
14. Baggio LL, Huang Q, Brown TJ, Drucker DJ. A recombinant human glucagon-like peptide (GLP)-1-albumin protein (albugon) mimics peptidergic activation of GLP-1 receptor-dependent pathways coupled with satiety, gastrointestinal motility, and glucose homeostasis. *Diabetes*. 2004;53(9):2492–2500.
15. Baggio LL, Huang Q, Brown TJ, Drucker DJ. Oxyntomodulin and glucagon-like peptide-1 differentially regulate murine food intake and energy expenditure. *Gastroenterology*. 2004;127(2):546–558.
16. Turton MD, et al. A role for glucagon-like peptide-1 in the central regulation of feeding. *Nature*. 1996; 379(6560):69–72.
17. Meeran K, et al. Repeated intracerebroventricular administration of glucagon-like peptide-1-(7-36) amide or exendin-(9-39) alters body weight in the rat. *Endocrinology*. 1999;140(1):244–250.
18. Baggio LL, Huang Q, Cao X, Drucker DJ. The long-acting albumin-exendin-4 GLP-1R agonist CJC-1134 engages central and peripheral mechanisms regulating glucose homeostasis. *Gastroenterology*. 2008; 134(4):1137–1147.
19. Rosenstock J, Reusch J, Bush M, Yang F, Stewart M. Potential of albiglutide, a long-acting GLP-1 receptor agonist, in type 2 diabetes: a randomized controlled trial exploring weekly, biweekly, and monthly dosing. *Diabetes Care*. 2009;32(10):1880–1886.
20. Williams DL. Minireview: finding the sweet spot: peripheral versus central glucagon-like peptide 1 action in feeding and glucose homeostasis. *Endocrinology*. 2009;150(7):2997–3001.
21. Burcelin R, Da Costa A, Drucker D, Thorens B. Glucose competence of the hepatoportal vein sensor requires the presence of an activated glucagon-like peptide-1 receptor. *Diabetes*. 2001;50(8):1720–1728.
22. Dardevet D, et al. Insulin secretion-independent effects of glucagon-like peptide 1 (GLP-1) on canine liver glucose metabolism do not involve portal vein GLP-1 receptors. *Am J Physiol Gastrointest Liver Physiol*. 2005;289(5):G806–G814.
23. Drucker DJ, Brubaker PL. Glucagon biosynthesis in fetal rat intestine. *Biomed Res*. 1988;9(suppl 3):29–32.
24. Jin S-LC, Han VKM, Simmons JG, Towle AC, Lauder JM, Lund PK. Distribution of glucagonlike peptide 1 (GLP-1), glucagon, and glicentin in the rat brain: An immunocytochemical study. *J Comp Neurol*. 1988;271(4):519–532.
25. Larsen PJ, Tang-Christensen M, Holst JJ, Orskov C. Distribution of glucagon-like peptide-1 and other preproglucagon-derived peptides in the rat hypothalamus and brainstem. *NeuroScience*. 1997; 77(1):257–270.
26. Knauf C, et al. Brain glucagon-like peptide-1 increases insulin secretion and muscle insulin resistance to favor hepatic glycogen storage. *J Clin Invest*. 2005; 115(12):3554–3563.
27. Sandoval DA, Bagnol D, Woods SC, D'Alessio DA, Seeley RJ. Arcuate glucagon-like peptide 1 receptors regulate glucose homeostasis but not food intake. *Diabetes*. 2008;57(8):2046–2054.
28. Nakabayashi H, Nishizawa M, Nakagawa A, Takeda R, Niijima A. Vagal hepatopancreatic reflex effect evoked by intraportal appearance of tGLP-1. *Am J Physiol*. 1996;271(5 Pt 1):E808–E813.
29. Vahl TP, et al. Glucagon-like peptide-1 (GLP-1) receptors expressed on nerve terminals in the portal vein mediate the effects of endogenous GLP-1 on glucose tolerance in rats. *Endocrinology*. 2007; 148(10):4965–4973.
30. Stoffers DA, Heller RS, Miller CP, Habener JF. Developmental expression of the homeodomain protein IDX-1 in mice transgenic for an IDX-1 promoter/lacZ transcriptional reporter. *Endocrinology*. 1999;140(11):5374–5381.
31. Drucker DJ, Philippe J, Mojsov S, Chick WL, Habener JF. Glucagon-like peptide I stimulates insulin gene expression and increases cyclic AMP levels in a rat islet cell line. *Proc Natl Acad Sci U S A*. 1987; 84(10):3434–3438.
32. Edwards CM, et al. Glucagon-like peptide 1 has a physiological role in the control of postprandial glucose in humans: studies with the antagonist exendin 9- 39. *Diabetes*. 1999;48(1):86–93.
33. Scrocchi LA, et al. Glucose intolerance but normal satiety in mice with a null mutation in the glucagon-like peptide receptor gene. *Nature Med*. 1996; 2(11):1254–1258.
34. Ali S, Lamont BJ, Charron MJ, Drucker DJ. Dual elimination of the glucagon and GLP-1 receptors in mice reveals plasticity in the incretin axis. *J Clin Invest*. 2011;121(5):1917–1929.
35. Hansotia T, et al. Double incretin receptor knockout (DIRKO) mice reveal an essential role for the enteroinsular axis in transducing the glucoregulatory actions of DPP-IV inhibitors. *Diabetes*. 2004; 53(5):1326–1335.
36. Maida A, Lamont BJ, Cao X, Drucker DJ. Metformin regulates the incretin receptor axis via a pathway dependent on peroxisome proliferator-activated receptor-alpha in mice. *Diabetologia*. 2011; 54(2):339–349.
37. Yamamoto H, et al. Glucagon-like peptide-1-responsive catecholamine neurons in the area postrema link peripheral glucagon-like peptide-1 with central autonomic control sites. *J Neurosci*. 2003; 23(7):2939–2946.
38. Yamamoto H, et al. Glucagon-like peptide-1 receptor stimulation increases blood pressure and heart rate and activates autonomic regulatory neurons. *J Clin Invest*. 2002;110(1):43–52.
39. Rankin MM, Kushner JA. Adaptive beta-cell proliferation is severely restricted with advanced age. *Diabetes*. 2009;58(6):1365–1372.
40. Xu G, Stoffers DA, Habener JF, Bonner-Weir S. Exendin-4 stimulates both beta-cell replication and neogenesis, resulting in increased beta-cell mass and improved glucose tolerance in diabetic rats. *Diabetes*. 1999;48(12):2270–2276.
41. Koehler JA, Baggio LL, Lamont BJ, Ali S, Drucker DJ. GLP-1 receptor activation modulates pancreatitis-associated gene expression but does not modify the susceptibility to experimental pancreatitis in mice. *Diabetes*. 2009;58(9):2148–2161.
42. Simonsen L, et al. Exendin-4, but not dipeptidyl peptidase IV inhibition, increases small intestinal mass in GK rats. *Am J Physiol Gastrointest Liver Physiol*. 2007;293(1):G288–G295.
43. Tschen SI, Dhawan S, Gurlo T, Bhushan A. Age-dependent decline in beta cell proliferation restricts the capacity of beta cell regeneration in mice. *Diabetes*. 2009;58(6):1312–1320.
44. Merchenthaler I, Lane M, Shughrue P. Distribution of pre-pro-glucagon and glucagon-like peptide-1 receptor messenger RNAs in the rat central nervous system. *J Comp Neurol*. 1999;403(2):261–280.
45. Nakagawa A, et al. Receptor gene expression of glucagon-like peptide-1, but not glucose-dependent insulinotropic polypeptide, in rat nodose ganglion cells. *Auton Neurosci*. 2004;110(1):36–43.
46. Nishizawa M, et al. Effect of intraportal glucagon-like peptide-1 on glucose metabolism in conscious dogs. *Am J Physiol Endocrinol Metab*. 2003; 284(5):E1027–E1036.
47. Ionut V, Hucking K, Liberty IF, Bergman RN. Synergistic effect of portal glucose and glucagon-like peptide-1 to lower systemic glucose and stimulate counter-regulatory hormones. *Diabetologia*. 2005; 48(5):967–975.
48. Ionut V, Zheng D, Stefanovski D, Bergman RN.

Exenatide can reduce glucose independent of islet hormones or gastric emptying. *Am J Physiol Endocrinol Metab*. 2008;295(2):E269–E277.
49. Drucker DJ, Asa S. Glucagon gene expression in vertebrate brain. *J Biol Chem*. 1988;263(27):13475–13478.
50. Shimizu I, Hirota M, Ohboshi C, Shima K. Identification and localization of glucagon-like peptide-1 and its receptor in rat brain. *Endocrinology*. 1987; 121(3):1076–1082.
51. Kinzig KP, et al. CNS glucagon-like peptide-1 receptors mediate endocrine and anxiety responses to interoceptive and psychogenic stressors. *J Neurosci*. 2003;23(15):6163–6170.
52. Nogueiras R, et al. Direct control of peripheral lipid deposition by CNS GLP-1 receptor signaling is mediated by the sympathetic nervous system and blunted in diet-induced obesity. *J Neurosci*. 2009;29(18):5916–5925.
53. Cabou C, et al. Brain glucagon-like peptide-1 regulates arterial blood flow, heart rate, and insulin sensitivity. *Diabetes*. 2008;57(10):2577–2587.
54. Drucker DJ, Nauck MA. The incretin system: glucagon-like peptide-1 receptor agonists and dipeptidyl peptidase-4 inhibitors in type 2 diabetes. *Lancet*. 2006;368(9548):1696–1705.
55. Edvell A, Lindstrom P. Initiation of increased pancreatic islet growth in young normoglycemic mice (Umea +/?). *Endocrinology*. 1999;140(2):778–783.
56. Buteau J, Roduit R, Susini S, Prentki M. Glucagon-like peptide-1 promotes DNA synthesis, activates phosphatidylinositol 3-kinase and increases transcription factor pancreatic and duodenal homeobox gene 1 (PDX-1) DNA binding activity in beta (INS-1)-cells. *Diabetologia*. 1999;42(7):856–864.
57. Hansotia T, et al. Extrapancreatic incretin receptors modulate glucose homeostasis, body weight, and energy expenditure. *J Clin Invest*. 2007;117(1):143–152.
58. Bustin SA. Absolute quantification of mRNA using real-time reverse transcription polymerase chain reaction assays. *J Mol Endocrinol*. 2000;25(2):169–193.
59. Livak KJ, Schmittgen TD. Analysis of relative gene expression data using real-time quantitative PCR and the 2(-Delta Delta C(T)) Method. *Methods*. 2001; 25(4):402–408.
60. Lamont BJ, Drucker DJ. Differential anti-diabetic efficacy of incretin agonists vs. DPP-4 inhibition in high fat fed mice. *Diabetes*. 2008;57(1):190–198.
61. Kwan EP, Xie L, Sheu L, Ohtsuka T, Gaisano HY. Interaction between Munc13-1 and RIM is critical for glucagon-like peptide-1 mediated rescue of exocytotic defects in Munc13-1 deficient pancreatic beta-cells. *Diabetes*. 2007;56(10):2579–2588.
62. Flock G, Holland D, Seino Y, Drucker DJ. GPR119 Regulates Murine Glucose Homeostasis Through Incretin Receptor-Dependent and Independent Mechanisms. *Endocrinology*. 2011;152(2):374–383.
63. Strommer L, et al. Delayed gastric emptying and intestinal hormones following pancreatoduodenectomy. *Pancreatology*. 2005;5(6):537–544.
64. Lee J, Martin E, Paulino G, de Lartigue G, Raybould HE. Effect of ghrelin receptor antagonist on meal patterns in cholecystokinin type 1 receptor null mice. *Physiol Behav*. 2011;103(2):181–187.
65. Franklin K, Paxinos G. *The Mouse Brain In Sterotaxic Coordinates*. San Diego, California, USA: Academic Press; 1997.